The Astronomical Journal, 139:1168–1177, 2010 March doi:10.1088/0004-6256/139/3/1168

Ca II TRIPLET SPECTROSCOPY OF SMALL MAGELLANIC CLOUD RED GIANTS. II. ABUNDANCES FOR A SAMPLE OF FIELD STARS

M. C. Parisi[1], D. Geisler[2], A. J. Grocholski[3], J. J. Clariá[1], and A. Sarajedini[4]
[1] Observatorio Astronómico, Universidad Nacional de Córdoba Laprida 854, Córdoba, CP 5000, Argentina; celeste@oac.uncor.edu, claria@oac.uncor.edu
[2] Departamento de Astronomía, Universidad de Concepción Casilla 160-C, Concepción, Chile; dgeisler@astro-udec.cl
[3] Space Telescope Science Institute 3700 San Martin Drive, Baltimore, MD 21218, USA; aarong@stsci.edu
[4] Department of Astronomy, University of Florida, P.O. Box 112055, Gainesville, FL 32611, USA; ata@astro.ufl.edu
Received 2009 July 20; accepted 2009 November 19; published 2010 February 11

ABSTRACT

We have obtained metallicities of ∼360 red giant stars distributed in 15 Small Magellanic Cloud (SMC) fields from near-infrared spectra covering the Ca II triplet lines using the VLT + FORS2. The errors of the derived [Fe/H] values range from 0.09 to 0.35 dex per star, with a mean of 0.17 dex. The metallicity distribution (MD) of the whole sample shows a mean value of [Fe/H] = −1.00 ± 0.02, with a dispersion of 0.32 ± 0.01, in agreement with global mean [Fe/H] values found in previous studies. We find no evidence of a metallicity gradient in the SMC. In fact, on analyzing the MD of each field, we derived mean values of [Fe/H] = −0.99 ± 0.08 and [Fe/H] = −1.02 ± 0.07 for fields located closer and farther than 4° from the center of the galaxy, respectively. In addition, there is a clear tendency for the field stars to be more metal-poor than the corresponding cluster they surround, independent of their positions in the galaxy and of the clusters' age. We argue that this most likely stems from the field stars being somewhat older and therefore somewhat more metal-poor than most of our clusters.

Key words: galaxies: stellar content – Magellanic Clouds – stars: abundances

Online-only material: color figure, machine-readable and VO tables

1. INTRODUCTION

Local Group galaxies have long been recognized as being excellent laboratories for understanding the star formation and the chemical enrichment histories of dwarf galaxies. In particular, the Small Magellanic Cloud (SMC) and its companion, the Large Magellanic Cloud (LMC), are close enough to resolve their oldest individual stars, thus allowing a detailed determination of the full range of ages as well as metallicities. This permits a better understanding of the formation and evolution of this kind of galaxy. Unfortunately, the SMC has not been studied as thoroughly as the LMC. Our knowledge about the chemical evolution history of the SMC mainly comes from the study of its cluster system. Da Costa & Hatzidimitriou (1998) and Piatti et al. (2001, 2005, 2007a, 2007b, 2007c), among others, have tried to derive the age–metallicity relation (AMR) of this galaxy on the basis of Ca II triplet spectroscopic and photometric studies, respectively. Recently, Parisi et al. (2009, hereafter Paper I) applied the Ca II triplet method (Cole et al. 2004; Grocholski et al. 2006) to 15 SMC clusters. The AMR derived in Paper I shows evidence for three phases: a very early (>11 Gyr) phase in which the metallicity reached [Fe/H] ∼−1.2; a long intermediate phase from ∼10–3 Gyr in which the metallicity only slightly increased although a number of clusters formed, and a final phase from 3–1 Gyr ago in which the rate of enrichment was remarkably faster. They find overall good agreement with the model of Pagel & Tautvaišienė (1998) which assumes a burst of star formation at 4 Gyr.

There are just a few studies in which the chemical enrichment history of the SMC is analyzed from field stars. Dolphin et al. (2001), based on *VI* photometry of a field in the outer SMC, found a metallicity of [Fe/H] = −1.3 ± 0.3 for the oldest stars, which increased up to [Fe/H] = −0.7 ± 0.2 by 1–2 Gyr ago. Harris & Zaritsky (2004) derived the chemical enrichment history in the central area of the SMC based on *UBVI* photometry from their Magellanic Cloud Photometric Survey. They found that the stars formed until ∼3 Gyr ago have a mean abundance [Fe/H] ∼−1 rising monotonically to a present value of [Fe/H] ∼−0.4. Using Ca II triplet (CaT) spectroscopy of ∼350 red giant branch stars in 13 SMC fields, Carrera et al. (2008) found that in the innermost fields the average metallicity is [Fe/H] ∼−1.0. However, this value decreases in the outermost regions, suggesting a metallicity gradient. They also showed that this metallicity gradient is related to an age gradient in the sense that the stars concentrated in the central regions are generally younger. Carrera et al.'s (2008) study supports the results of Piatti et al. (2007a, 2007b) who also came to a similar conclusion. However, no evidence of such a gradient was found in Paper I, which covered a much wider range in galactocentric distance. The recent work of Cioni (2009), using the C/M ratio of asymptotic giant branch (AGB) stars to derive metallicity, also supports a negligible gradient.

It is interesting to compare the metallicity of the clusters and of their surrounding fields, especially to understand the possible formation mechanisms of these different kinds of SMC populations. According to Westerlund (1997), there is no reason to expect large differences in abundances between clusters and field stars although several recent studies point in the opposite direction. For example, Piatti et al. (2007a), analyzing metallicities and ages of a sample of 42 clusters, showed that young clusters are at least 0.3 dex more metal-rich than the population of surrounding field stars, presumably of similar age. They interpret this result as evidence that most field stars are formed either from remnant gas clouds from star cluster formation or from disrupted clusters, in agreement with the scenario of Chandar et al. (2006). Nonetheless, Piatti et al. (2007c) suggested, after analyzing the AMR of clusters and field stars, that these two populations started to undergo similar chemical enrichment histories the last couple of gigayears, but

their chemical evolution was clearly different in the period between 4 and 10 Gyr ago.

In a recent paper, Tsujimoto & Bekki (2009) argued that there is a dip in the AMR of both field and cluster stars in the SMC around 7.5 Gyr ago. They apply chemical evolution models to suggest that this dip was caused by a major merger of the SMC with a metal-poor, gas-rich galaxy at this epoch, and find reasonable fits between their models and the observed AMR.

In this paper, we examine the metallicities of field stars surrounding a sample of star clusters of the SMC. As noted above, our current knowledge of the chemical evolution of this neighboring galaxy is very limited. In order to definitively determine the existence and nature of any gradient, the likelihood of a past merger, differences in the AMR between cluster and field stars, and other key questions requires a substantial improvement in both data quantity and quality. The CaT technique is a very efficient, sensitive and well-calibrated metallicity index for giant stars. Simultaneously with the cluster giants discussed in Paper I, we observed a large number of field giants surrounding each cluster. This data set represents an important step in the above direction. In Section 2, we describe our field star sample, while in Section 3 the spectroscopic observations and reduction procedures are detailed. In Sections 4 and 5, we present the radial velocities (RVs) and equivalent width (EW) measurements and the metallicity derivation of the star fields, respectively. In Section 6, we discuss the results obtained from the metallicities. Finally, in Section 7 we summarize our main findings and conclusions.

2. FIELD SAMPLE

Recently, we determined metallicities and RVs for a sample of SMC clusters based on CaT spectroscopy of red giant stars (Paper I). As part of Program 076.B-0553, *V*- and *I*-band pre-images of our targets were taken by ESO Paranal staff in 2005 August. Clusters were centered on the upper (master) CCD, while the lower (secondary) CCD was used to observe only field stars. Target fields were selected trying to cover as wide an area and radial range in the galaxy as possible in order to search for any global effects such as gradients. Figure 1 of Paper I shows the positions of our target sample.

The pre-images were processed within IRAF[5] and stars were identified and photometered using the aperture photometry routines in DAOPHOT (Stetson 1987). Stars were cataloged using the FIND routine in DAOPHOT and photometered with an aperture radius of 3 pixels. The *V*- and *I*-band data were matched to form colors.

The selection of the cluster spectrocopic targets is described in detail in Paper I. In brief, they were chosen based on the instrumental color–magnitude diagram (CMD) by selecting stars located along the cluster giant branch. At the same time, we also selected as many stars as possible on the cluster chip which also appeared to be giants falling outside the cluster radius (after first maximizing the number of cluster stars placed on slits) in order to explore the field star chemistry and kinematics. We similarly selected as many field giants as possible from the secondary chip.

Field stars on the secondary chip plus the stars of the master chip which were rejected as cluster members according to our membership discrimination method (see Section 6 of Paper I for more details) are taken as the selected sample for this study. We carefully checked the metallicities and RVs of the field stars taken from the master chip to make sure that they are incompatible with the corresponding cluster values. This reaffirmed our confidence in the absence of star cluster contamination. The secondary chip is located far enough from the master one to make any potential cluster contamination negligible.

The total field star sample amounts to ≈360 stars in 15 SMC fields. Table 1 lists the cluster equatorial coordinates. We named each field after the corresponding cluster.

Table 1
SMC Clusters

Cluster	R.A. (J2000.0) (h m s)	Decl. (J2000.0) (° ′ ″)
BS 121	01 04 22	−72 50 52
HW 47	01 04 04	−74 37 09
HW 84	01 41 28	−71 09 58
HW 86	01 42 22	−74 10 24
L 4	00 21 27	−73 44 55
L 5	00 22 40	−75 04 29
L 6	00 23 04	−73 40 11
L 7	00 24 43	−73 45 18
L 17	00 35 42	−73 35 51
L 19	00 37 42	−73 54 30
L 27	00 41 24	−72 53 27
L 72	01 03 53	−72 49 34
L 106	01 30 38	−76 03 16
L 108	01 31 32	−71 57 10
L 110	01 34 26	−72 52 28
L 111	01 35 00	−75 33 24

3. SPECTROSCOPIC OBSERVATIONS AND REDUCTIONS

The spectra of the program stars were obtained during 2005 November in service mode by the Very Large Telescope (VLT) staff, using the FORS2 spectrograph in mask exchange unit (MXU) mode. Our instrumental setup is discussed in Paper I, which can be referred to for a more detailed description. We used slits that were 1″ wide and 8″ long and single exposures of 900 s were obtained with a typical seeing less than 1″. The spectra have a dispersion of ∼0.85 Å pixel^{-1} (resolution of 2–3 Å) with a characteristic rms scatter of ∼0.06 Å and cover a range of ∼1600 Å in the region of the CaT (8498 Å, 8542 Å, and 8662 Å). Signal-to-noise ratio (S/N) values ranged from ∼10 to ∼70 pixel^{-1}. Calibration exposures, bias frames, and flat fields were also taken by the VLT staff.

We followed the image processing detailed in Paper I. In brief, the IRAF task *ccdproc* was used to fit and subtract the overscan region, trim the images, fix bad pixels, and flat field each image. We then corrected the images for distortions, which rectifies the image of each slitlet to a constant range in the spatial direction and then traces the sky lines along each slitlet and puts them perpendicular to the dispersion direction. We used the task *apall* to define the sky background and extract the stellar spectra onto one dimension. The tasks *identify, refspectra* and *dispcor* were used to calculate and apply the dispersion solution for each spectrum. Finally, the spectra were continuum-normalized by fitting a polynomial to the stellar continuum. In Figure 1, two examples of the final spectra in the CaT region can be observed.

[5] Image Reduction and Analysis Facility, distributed by the National Optical Astronomy Observatory, which is operated by the Association of Universities for Research in Astronomy, Inc., under contract with the National Science Foundation.

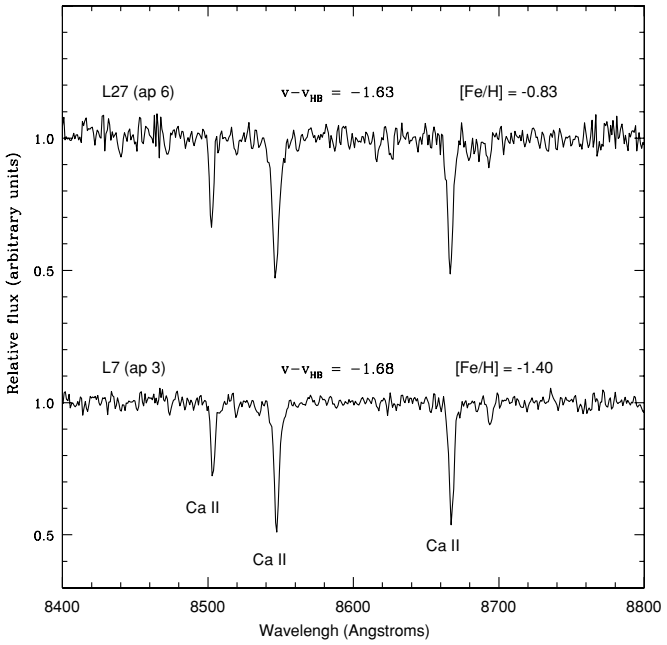

Figure 1. Sample continuum-normalized spectra of RGB stars in two fields of our sample. The three Ca T lines have been marked on the plot as well as the corresponding $v - v_{\rm HB}$ values and metallicities. These two stars have very similar $T_{\rm effs}$ and log g values. Thus, the difference in Ca II line strength illustrates their substantial metallicity difference.

4. RADIAL VELOCITY AND EQUIVALENT WIDTH MEASUREMENTS

Radial velocities of our target field stars are useful for analyzing the kinematics of the SMC and comparing our results with those obtained using other SMC objects such as star clusters, carbon stars, etc. Although the kinematic analysis is beyond the scope of this paper, the program used to measure the EW of the CaT lines requires knowledge of the RV to make the Doppler correction and to derive the CaT line centers.

To measure RVs of our program stars, we performed cross-correlations between their spectra and those of 32 bright Milky Way open and globular cluster template giants using the IRAF task *fxcor* (Tonry & Davis 1979). We used the template stars of Cole et al. (2004, hereafter C04) who observed these stars with a setup very similar to ours. The template spectra are listed in Section 4 of Paper I. *Fxcor* also makes the necessary correction to place the derived RV in the heliocentric reference frame. We adopted the average of the ensemble cross-correlation results as the heliocentric RV of a star, finding a typical standard deviation of $\sim$6 km s^{-1}.

Errors in centering the image in the spectrograph slit may lead to inaccuracies in determining RVs, as previous papers have shown (e.g., Irwin & Tolstoy 2002). We corrected these errors following the procedure described in Section 4 of Paper I. As shown in that section, the velocity corrections we have applied range from $|\Delta v| = 0$ to 27 km s^{-1}, and the typical error introduced in the RV turns out to be $\pm$4.5 km s^{-1}. This error, added in quadrature to the one resulting from the cross-correlation, yields a total error of 7.5 km s^{-1}, which has been adopted as the typical RV error (random + systematic) of an individual star.

To measure EWs we have used a previously written FORTRAN program (see C04 for details). We followed the procedure of Armandroff & Zinn (1988), described in detail in Section 4 of Paper I, on the basis of which we define continuum bandpasses on both sides of each CaT line, determine the "pseudo-continuum" for each line by a linear fit to the mean value in each pair of continuum windows and calculate the "pseudo-EW" by fitting a function to each CaT line in relation to the pseudo-continuum. We fit a Gaussian function to each CaT line in those spectra with S/N $<$ 20 and fit a composite function (Gaussian plus Lorentzian) to the spectra with S/N $>$ 20 (see Paper I for justification). We then corrected the Gaussian-only fit for the low S/N spectra according to Equation (2) of Paper I.

5. METALLICITIES

The relationship between the strengths of the CaT lines and stellar abundance has been calibrated by several studies. In all cases, the selected CaT index uses a linear combination of the EW of two or three individual Ca II lines to form the line strength index ΣW. Because our spectra are high enough quality that all three CaT lines can be measured, we adopted for ΣW the same definition adopted by C04, in which all three lines are used with equal weight, namely:

$$\Sigma W = EW_{8498} + EW_{8542} + EW_{8662}. \quad (1)$$

Theoretical and empirical studies have shown that effective temperature, surface gravity, and [Fe/H] all play a role in CaT line strengths (e.g., Jørgensen et al. 1992; Cenarro et al. 2002). However, Armandroff & Da Costa (1991) showed that there is a linear relationship between a star's absolute magnitude and ΣW for red giants of a given metallicity. Following previous authors, we define a reduced EW, W', to remove the effects of surface gravity and temperature on ΣW via its luminosity dependence:

$$W' = \Sigma W + \beta(V - V_{HB}), \quad (2)$$

in which the introduction of the difference between the visual magnitude of the star (V) and the cluster's horizontal branch/red clump ($V_{\rm HB}$) also removes any dependence on distance and interstellar reddening. Here, as our magnitudes are uncalibrated, we use v and $v_{\rm HB}$. The $v_{\rm HB}$ was derived from the corresponding cluster or field CMD, for stars on the master or secondary chip, respectively. In those cases where the red clump happened not to be clearly evident on the secondary chip (L 106, L 110, and L 111), we assume that the field $v_{\rm HB}$ is the same as that of the cluster located on the master chip. As Grocholski et al. (2006) discussed in detail, the use of an inappropriate $V - V_{\rm HB}$ can introduce systematic errors in the derived metallicities. Specifically, C04 and Koch et al. (2006) showed that the associated error in [Fe/H] is on the order of $\pm$0.05 dex but it can be as large as $\pm$0.1 dex, in extreme cases. Therefore, for these three fields, we have added an error of $\pm$0.1 dex in quadrature with the one corresponding to the metallicity calculation.

The value of β has been investigated by previous authors. We prefer to adopt the value obtained by C04, i.e., $\beta = 0.73 \pm 0.04$, because C04's instrumental setup was very similar to ours, and they investigated this parameter in depth. As discussed in detail in Grocholski et al. (2006), it is not necessary to make any corrections for age effects. Rutledge et al. (1997) showed that there is a linear relationship between the reduced EW and metallicity on the Carretta & Gratton (1997) abundance scale for globular clusters of the Milky Way. C04 extended this calibration to a wider range of ages (2.5 Gyr $\leqslant$ age $\leqslant$ 13 Gyr) and metallicities ($-2.0 \leqslant$ [Fe/H] $\leqslant -0.2$) by combining the metallicity scales of Carretta & Gratton (1997) and Friel et al. (2002) for globular and open clusters, respectively. Further

Table 2
Position and Measured Values for Field Stars

ID	R.A. (J2000.0) (h m s)	Decl. (J2000.0) (° ′ ″)	$v - v_{HB}$ (mag)	ΣW (Å)	$\sigma_{\Sigma W}$ (Å)	[Fe/H]	$\sigma_{[Fe/H]}$
BS 121M-1	01 04 06.51	−72 51 09.61	−0.40	5.89	0.32	−0.939	0.150
BS 121M-3	01 04 11.76	−72 51 13.40	−0.21	5.27	0.42	−1.114	0.177
BS 121M-6	01 04 23.74	−72 50 50.82	−0.04	4.01	0.38	−1.525	0.158
BS 121M-8	01 04 22.44	−72 51 29.66	−1.18	5.59	0.11	−1.253	0.098
BS 121M-9	01 04 30.69	−72 50 57.06	−1.25	6.29	0.12	−1.018	0.105

(This table is available in its entirety in machine-readable and Virtual Observatory (VO) forms in the online journal. A portion is shown here for guidance regarding its form and content.)

extensions of the calcium triplet calibrations are provided by Battaglia et al. (2008) (down to −2.5 dex) and by Carrera et al. (2007) (to +0.5 dex and 0.25 Gyr). We adopted the C04 relationship,

$$[Fe/H] = (-2.966 \pm 0.032) + (0.362 \pm 0.014)W', \quad (3)$$

to derive the metallicities of our field star sample. We estimate that the total metallicity error (random + systematic) per star ranges from 0.09 to 0.35 dex, with a mean of 0.17 dex. In Table 2, we list the information for the individual stars. Columns 1–3 show the identification of the star, right ascension (R.A.) and declination (decl.), respectively. Table 2 also lists $v - v_{HB}$ in Column 4, ΣW and its error in Columns 5 and 6 and metallicity and its error in Columns 7 and 8. We considered only those stars with $50 < RV < 250$ km s^{-1} as SMC members (Harris & Zaritsky 2006).

We emphasize that this analysis followed the identical procedure used and detailed in Paper I for the cluster giants, assuring that the derived metallicities are completely comparable.

6. METALLICITY ANALYSIS

The field star metallicity distribution (hereafter MD) in a galaxy is an extremely useful tool to investigate its overall chemical evolution. Figure 2 shows the MD of all the field stars in our sample as well as the (quite good) Gaussian fit. We derived a mean metallicity of $[Fe/H] = -1.00 \pm 0.02$ with a dispersion of 0.32 ± 0.01, in excellent agreement with the global mean value of −1.0 found by Carrera et al. (2008) from CaT spectra of a large number of field giants. Our derived mean metallicity also shows very good agreement with the mean value of $[Fe/H] = -0.96$ we found in Paper I from CaT spectra of star clusters.

There are previous hints in the literature about the existence of a metallicity gradient in the SMC. Piatti et al. (2007a, 2007b) found that the mean metallicity values and the respective metallicity dispersions of their cluster sample tend to be higher for the clusters located within 4° from the SMC center than for those situated outside this radius. Recently, Carrera et al. (2008) studied ∼350 red giant stars in 13 fields distributed from ∼1° to ∼4° from the center, using CaT spectroscopy. They found a mean metallicity of [Fe/H] ∼−1.0 in the *innermost* SMC fields, with the mean decreasing in the outermost regions, reaching [Fe/H] ∼−1.6 at ∼4° radius from the SMC center. They also found a relationship between this metallicity gradient and the age gradient in the sense that the youngest stars, concentrated in the central regions, are the most metal-rich. However, in Paper I we found no clear evidence of any true metallicity gradient in the SMC cluster system from data which extend to regions further from the center than the outermost Carrera fields. Cioni

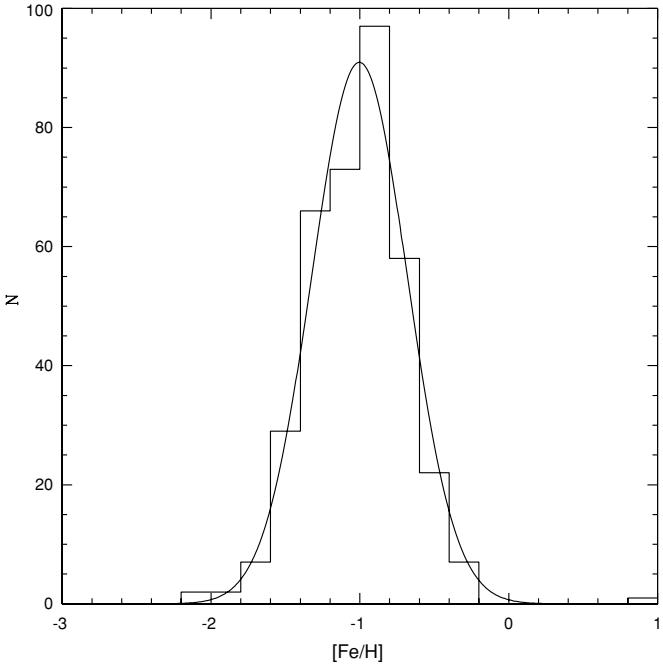

Figure 2. Metallicity distribution of all field stars of our sample. The corresponding Gaussian fit is shown by the solid line.

(2009) derived the [Fe/H] of 7653 SMC AGB stars within an area of 20° × 20°. Her results are in agreement with the lack of a metallicity gradient in this galaxy. In addition, her mean metallicity value of -1.12 ± 0.03 is also in good agreement with our field value within their dispersions.

With the aim of testing the possible existence of a metallicity gradient from our field stars, we fit Gaussian functions to the MD of each of our fields. The resulting MDs together with their respective Gaussian fits are shown in Figures 3–6. Since the Gaussian fits of the L 7 (Figure 4(d)) and L 17 (Figure 5(a)) fields were not satisfactory, we decided to use the median metallicity in each case. The resulting median metallicities and standard errors of the median (between brackets) are −1.01 (0.07) and −0.89 (0.06) for L 7 and L 17, respectively. In the L 106 field, we do not have a sample of stars large enough to fit a Gaussian to the MD (Figure 5(d)). The mean value of this small sample is $[Fe/H] = -0.92 \pm 0.16$ (standard error of the mean). From a statistical point of view, the L106 field sample is too small to conclude that the mean metallicity value is more appropriate than the median value. We decided to use the mean value for the subsequent analysis; however, it is necessary to keep in mind that the median metallicity for this sample is −0.77. The remaining MDs exhibit reasonably good single Gaussian fits. In Table 3, we list field ID in Column 1, the number n of stars belonging

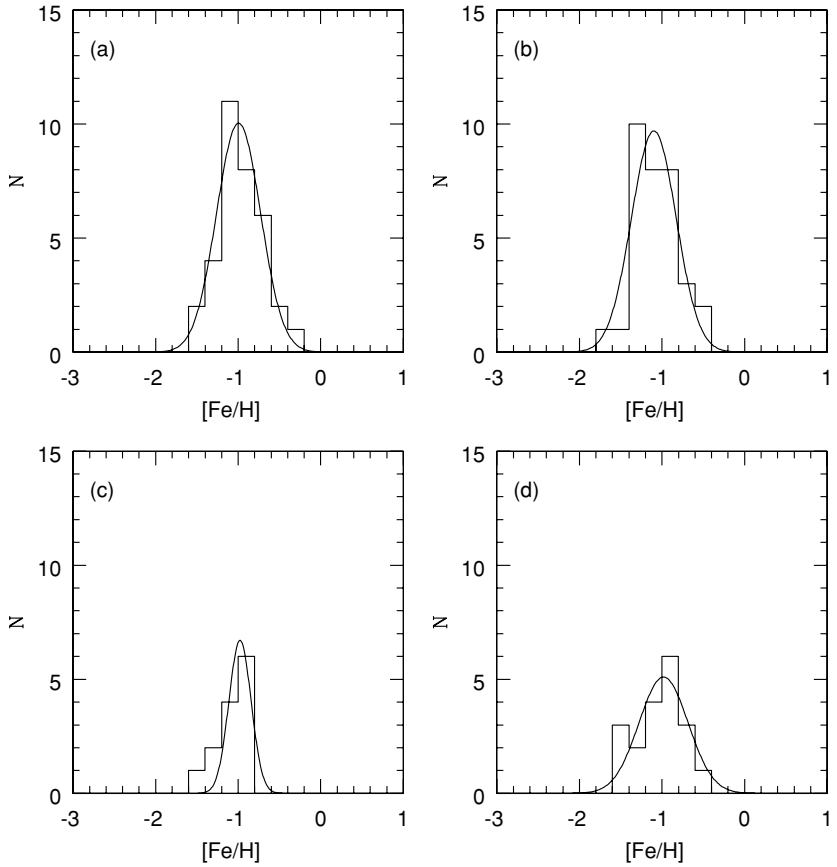

Figure 3. Metallicity distributions of the field stars surrounding the clusters: (a) BS 121, (b) HW 47, (c) HW 84, and (d) HW 86. The solid curves show the corresponding Gaussian fit.

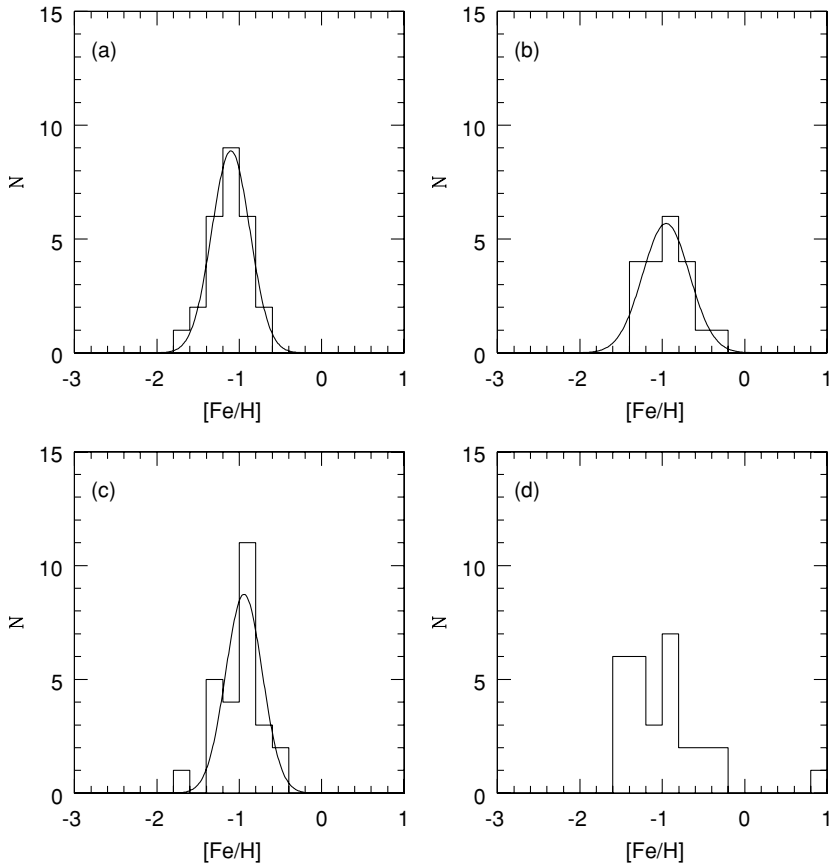

Figure 4. Same as in Figure 3 for the field stars surrounding the clusters: (a) L 4, (b) L 5, (c) L 6, and (d) L 7.

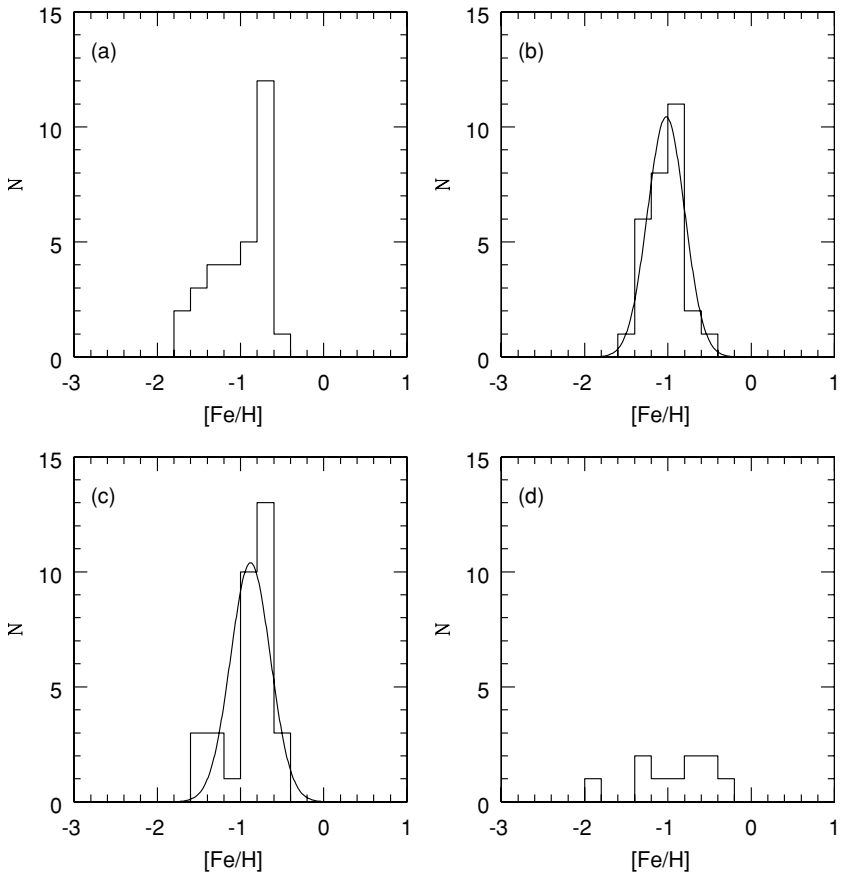

Figure 5. Same as in Figure 3 for field stars surrounding the clusters: (a) L 17, (b) L 19, (c) L 27, and (d) L 106.

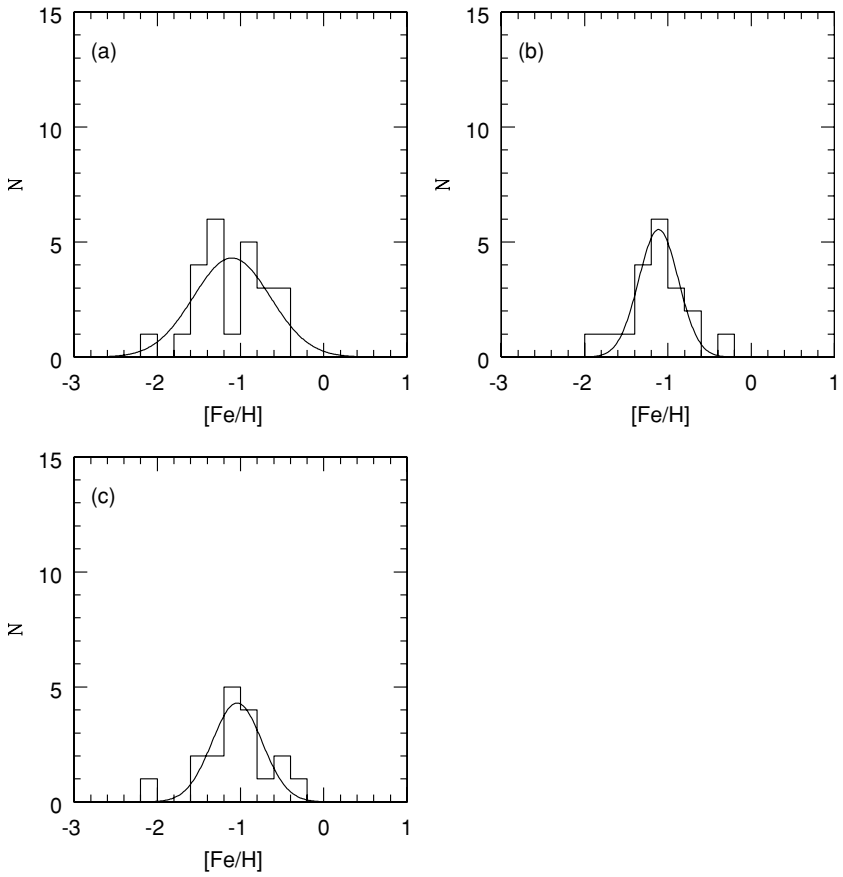

Figure 6. Same as in Figure 3 for the field stars surrounding the clusters: (a) L 108, (b) L 110, and (c) L 111.

Table 3
SMC Fields Results

ID	n	$[\bar{Fe}/H]$	$\sigma_{[\bar{Fe}/H]}$	a
BS 121	34	-0.99 ± 0.02	0.27 ± 0.02	1.496
HW 47	33	-1.10 ± 0.02	0.27 ± 0.03	3.502
HW 84	13	-0.98 ± 0.01	0.13 ± 0.02	5.513
HW 86	19	-0.98 ± 0.03	0.29 ± 0.03	7.345
L 4	26	-1.10 ± 0.01	0.23 ± 0.005	3.265
L 5	20	-0.95 ± 0.02	0.29 ± 0.02	3.092
L 6	26	-0.94 ± 0.03	0.22 ± 0.03	3.124
L 7	29	-1.01 ± 0.07	...	2.888
L 17	31	-0.89 ± 0.06	...	1.718
L 19	29	-1.02 ± 0.02	0.22 ± 0.02	1.564
L 27	33	-0.88 ± 0.05	0.24 ± 0.04	1.392
L 106	10	-0.92 ± 0.16	...	7.877
L 108	24	-1.10 ± 0.08	0.46 ± 0.08	4.460
L 110	19	-1.11 ± 0.02	0.24 ± 0.02	5.323
L 111	18	-1.04 ± 0.04	0.30 ± 0.04	7.830

to the field in Column 2, the mean metallicity and metallicity dispersions with their respective errors in Columns 3 and 4 and the semimajor axis a (discussed below) in Column 5.

In order to look into the possible existence of a metallicity gradient in the SMC, the orientation of the galaxy and projection effects must first be addressed. The orientation is so far poorly determined, and the galaxy is markedly elongated along the line of sight, making the determination of true galactocentric distances difficult to perform. We then followed, as in Paper I, the procedure described by Piatti et al. (2007a), according to which we adopted an elliptical coordinate system (Figure 1, Paper I) and computed for each field the value of the semimajor axis, a, which an ellipse would have under the following conditions: (1) if it were centered on the SMC center, (2) if it were aligned with the bar, (3) had a b/a ratio of 1/2, and (4) if one point of the trajectory coincided with the field position. Then, we use the a value as a surrogate for the true galactocentric distance.

In Figure 7, we plot the metallicity versus the semimajor axis a value for our field sample (filled circles) where it is evident that no clear trend is present. We divided our field sample into two regions: *inner* and *outer* 4° from the SMC center, as was done in Piatti et al. (2007a, 2007b) and in Paper I. In Figure 7, there are nine fields in the *inner* group and six fields in the *outer* group. We found a mean metallicity value of [Fe/H] = −0.99 for the *inner* group and [Fe/H] = −1.02 for the *outer* one (standard deviations of 0.08 and 0.07, respectively). This result reinforces the conclusion reached in Paper I in which very similar mean metallicity values of -0.94 ± 0.19 (standard deviation—15 clusters) and -1.00 ± 0.21 (10 clusters) were found for clusters in the *inner* and *outer* regions, respectively. The cluster sample of Paper I is also included in Figure 7 (open circles and triangles). We remind the reader that in Paper I we supplemented our 15 clusters observed with FORS2 (open circles in Figure 7) with 10 additional clusters from the literature (Da Costa & Hatzidimitriou 1998; Glatt et al. 2008; Gonzalez & Wallerstein 1999) plotted as triangles. We showed in Paper I that the lack of a metallicity gradient cannot be caused by an age gradient effect since the mean ages and standard deviations are 3.1 and 1.9 Gyr for the *inner* clusters and 4.4 and 3.4 Gyr for the *outer* ones. As already mentioned, Carrera et al. (2008) suggested the existence of such a gradient. In order to compare their results with ours, we have included in Figure 7 the fields studied by those authors (squares). As can be seen, their evidence for the existence of a metallicity gradient is completely dependent on

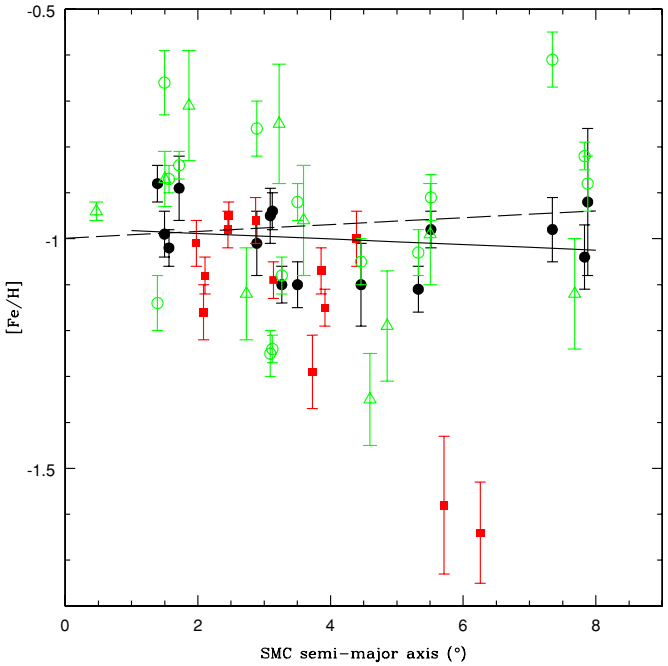

Figure 7. Mean metallicity vs. semimajor axis a for the fields of our sample (filled circles). Open circles represent our CaT cluster sample studied in Paper I, and empty triangles correspond to the additional cluster sample also included in Paper I. Fields of Carrera et al. (2008) are represented by squares. Error bars correspond to the standard error of the mean except for the extended cluster sample in which errors are the ones quoted in the corresponding paper (Da Costa & Hatzidimitriou 1998; Glatt et al. 2008; Gonzalez & Wallerstein 1999). The solid line shows the linear fit for our field sample while the dashed one corresponds to the linear fit of the complete sample (fields plus clusters in Paper I).

(A color version of this figure is available in the online journal.)

the two outermost fields. There are now 7 fields and 10 clusters located in the same outer region, whose mean metallicity is indistinguishable from the global value of [Fe/H] = −1.0. No other data points support such a low metallicity at any radius. In particular, the four clusters and three field points at even larger galactocentric distances are completely in agreement with all of the other points except the two outliers of Carrera. We believe that, from a statistical point of view, the absence of a metallicity gradient is more probable, as supported by Cioni (2009). In fact, the best-fit line for the data shows a clear tendency to flatness. The linear fit for our field sample turned out to be $[Fe/H] = -0.006 \pm 0.009 \times a - 0.98 \pm 0.04$ with a rms = 0.08 (solid line in Figure 7). The linear fit for the full sample (fields + clusters in Paper I) is $[Fe/H] = 0.007 \pm 0.012 \times a - 1.00 \pm 0.05$ with a rms = 0.14 (dashed line in Figure 7). Note that the error of Carrera et al.'s two outermost fields are the largest of their sample. As we have previously mentioned, Piatti et al. (2007a, 2007b) also found evidence for a metallicity gradient but it is important to keep in mind that the Piatti et al. values are based on Washington photometry, which typically has error bars of about 0.2 dex, but also includes a significant age correction for stars younger than 5 Gyr when using their standard giant branch technique.

Carrera et al. (2008) found evidence for a universal AMR. In the light of this, they argued that their metallicity gradient is not due to a variation of the AMR but to an age gradient, with the younger stars, which are the most metal-rich, concentrated in the central region of the galaxy. This result reinforces previous suggestions of Piatti et al. (2007a, 2007b) that the farther a

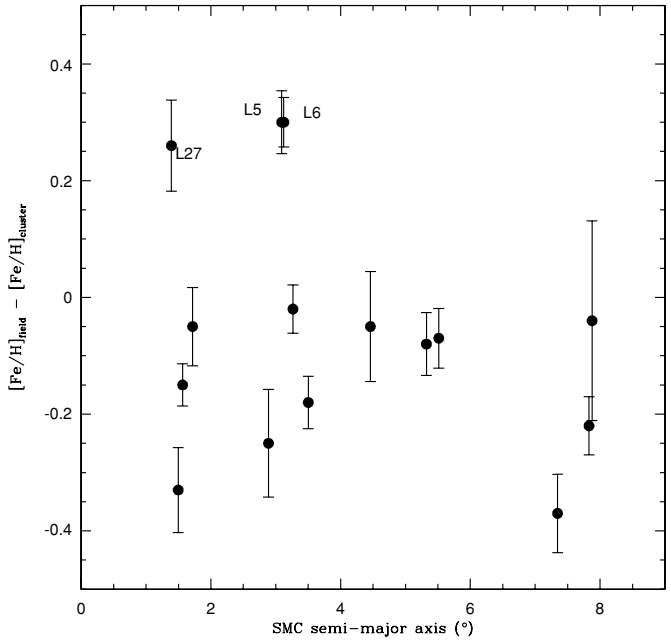

Figure 8. Difference between the metallicity of fields and that of the corresponding clusters vs. the semimajor axis *a*.

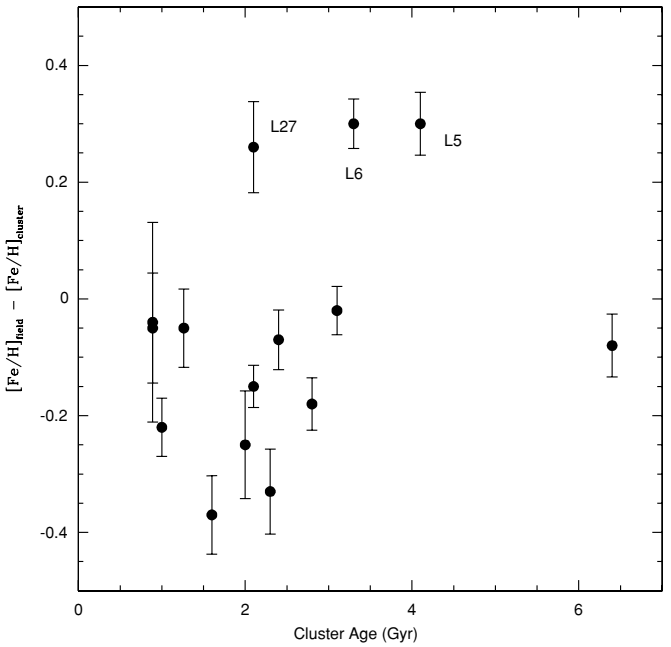

Figure 9. Difference between the metallicity of fields and that of the corresponding clusters vs. the cluster age.

cluster is from the center of the galaxy, the older and the more metal-poor it is. Then, if we accept that the AMR is in fact universal, the lack of a gradient of metallicity implies that there is not a variation of the age with the distance. It is interesting to note that Piatti et al. (2007c) found some relatively young clusters in the outer region which present a new twist for cluster formation in the SMC and its chemical evolution. They suggest that chemically enriched gas clouds can exist in the outermost portions of the galaxy. They do not discard the possibility that in the outer body ($a > 3\overset{\circ}{.}5$) of the SMC metallicity and age gradients could be somewhat negligible or non-existent. Also, Cioni (2009) suggests that during an encounter of the SMC with the LMC (∼3 Gy ago), star formation started to take place in the outer parts of the galaxy altering the [Fe/H] gradient. Zaritsky et al. (1994) and Friedli & Benz (1995) found that, while abundance gradients are common in spiral galaxies, the presence of a classical bar tends to weaken the gradient over a few dynamical timescales. This effect is seen in the LMC which has a stellar bar and shows no significant metallicity gradient (Olszewski et al. 1991; Geisler et al. 2003; Grocholski et al. 2006). Thus, the presence of a bar may explain the lack of a metallicity gradient in the SMC. It is also necessary to bear in mind that the true distance of each star in the field from the galaxy center is unknown. We assume the projected semimajor axis distance as the most appropriate coordinate system under the circumstances. In addition, the presence of a true (i.e., three-dimensional) radial gradient can be weakened in the transition to projected, two-dimensional coordinates.

To compare the clusters with their surrounding fields, we have plotted the difference between the metallicity of the field and that of the cluster versus the *a* value in Figure 8 and versus the cluster age in Figure 9. The adopted cluster age can be found in Table 4 of Paper I. Figures 8 and 9 show a clear tendency for most fields to be more metal-poor than the corresponding cluster, independently of their positions in the galaxy or the cluster age. There are, however, three exceptions to this behavior. The fields around L 5, L 6, and L 27 are all more metal-rich than their corresponding clusters. These three clusters are the most metal-

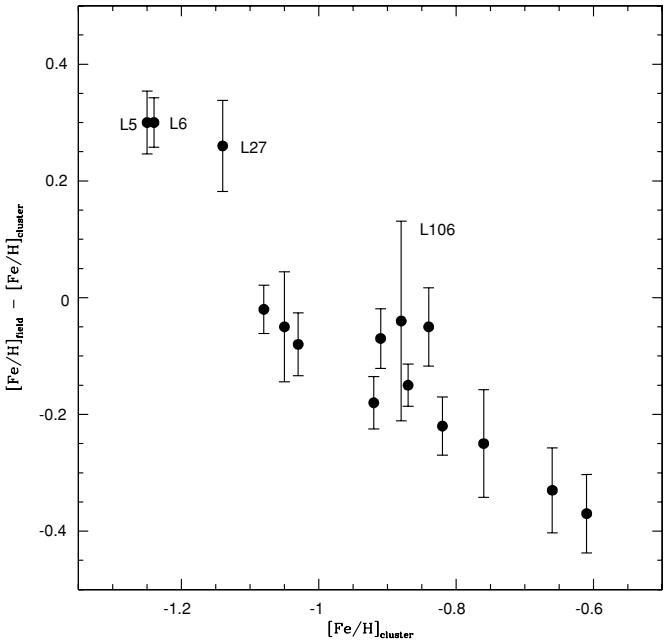

Figure 10. Difference between the metallicity of fields and that of the corresponding clusters vs. the cluster metallicity.

poor clusters in out CaT sample, and as such in Figure 10 we plot the metallicity difference between the fields and clusters as a function of the cluster metallicity. A clear trend is seen for the metallicity difference to decrease with increasing cluster metallicity and L 5, L 6, and L 27 are no longer outliers. We note that the large error associated with L 106 is due to the small number of field stars available.

One possible explanation for this trend is if clusters showed internal metallicity gradients and tidal disruption of the clusters stripped off the outer, more metal-poor stars. In this case, the resulting field stars surrounding the clusters would have a lower metallicity. However, this cannot explain the presence of field stars that are more metal-rich than their corresponding cluster, and given that the field stars have RVs that are distinct from

the clusters, we think that it is unlikely that the field stars are associated with the currently observed clusters. Also note that such metallicity gradients are not observed in any known clusters. Our preferred explanation is that the bulk of the field stars formed at an older epoch from most of the clusters we have observed, with the exact epoch dependent on which AMR we adopt. For example, we showed in Paper I that both the clusters and the field stars show only minor enrichment from approximately 10–3 Gyr ago, with an average [Fe/H] ~ -1, followed by substantial increase in metallicity after 3 Gyr. Since most of the clusters we observe are younger than $\sim$3 Gyr the observed AMR naturally explains the more metal-poor field stars if the bulk of the field is older than $\sim$3 Gyr. This is in agreement with the results of Sabbi et al. (2009), which suggest that the SMC actively formed field stars over a long time interval until about 2–3 Gyr ago. The existence of clusters like L 5, L 6, and L 27, which are the three intermediate-age, but relatively metal-poor clusters in our sample, is likely the result of minor mergers with metal-poor gas clouds which diluted the interstellar medium (ISM) in the SMC only locally, but may also be the result of a major merger that diluted the entire SMC (e.g., Tsujimoto & Bekki 2009). Finally, in this scenario the question arises as to why the field stars would be generally older than the bulk of the clusters. It is typically thought that most stars are formed in clusters (e.g., Lada & Lada 2003) and that field stars are the result of the subsequent dissolution of a majority of the clusters (e.g., Chandar et al. 2006; but see Bastian et al. 2009 for an opposing view), with only the more massive clusters surviving for an extended period of time. Thus, it is possible that prior to about $\sim$3 Gyr ago most of the clusters that formed in the SMC were of low enough mass to be easily dispersed into the field, whereas younger clusters were mostly massive enough to survive to the current time and thus not contribute a significant number of young stars to the field. This possibility is supported by dynamical simulations by Bekki et al. (2004) which suggest that the LMC and SMC had a very close encounter $\sim$4 Gyr ago that would have resulted in an increased rate of massive cluster formation in the Magellanic Clouds. Note, however, that the results of Besla et al. (2007) have brought into question whether or not the Magellanic Clouds have been interacting for an extended period of time.

Of course, information about the age of the fields is needed to perform a more reliable analysis of the chemical evolution history of field stars and to compare it with the evolution of the cluster system.

7. SUMMARY AND CONCLUSIONS

We used VLT + FORS2 to obtain near-infrared spectra of $\sim$360 giant stars distributed in 15 SMC fields, covering the spectral range that includes the three Ca II triplet lines. From these spectra we derived individual star RV and metallicity, applying the CaT technique (Cole et al. 2004; Grocholski et al. 2006; Parisi et al. 2009) in exactly the same manner as followed in Paper I for the targeted cluster. A mean error of 0.17 dex is achieved. The following summarizes the results of the analysis of these metallicities:

1. By fitting a Gaussian function to the whole sample, we found a mean value of [Fe/H] $= -1.00 \pm 0.02$ with a dispersion of 0.32 ± 0.01. This metallicity is in good agreement with the mean value of [Fe/H] $= -1.0$ found by Carrera et al. (2008) for field stars and [Fe/H] $= -0.96$ reported in Paper I for star clusters.
2. We also fit Gaussian functions to the metallicity distribution of each field in order to derive their mean metallicity and dispersion. There is practically no deviation from the value of [Fe/H] $= -1.0$ of the individual mean metallicities, which range from [Fe/H] $= -0.88$ to [Fe/H] $= -1.11$. The dispersions vary from 0.13 to 0.46.
3. By dividing our sample into *inner* and *outer* 4° from the SMC center, we found a mean metallicity (standard deviation) of [Fe/H] $= -0.99$ (0.08) and [Fe/H] $= -1.02$ (0.07) for the *inner* and *outer* regions, respectively. This result suggests that there is no metallicity gradient in the SMC, in agreement with the work of Cioni (2009) and with Paper I and contrary to the trend suggested by Carrera et al. (2008). Carrera et al. (2008) found evidence for a universal AMR and suggested that the metallicity gradient they derived is due to the presence of an age gradient in the galaxy. If we assume a universal AMR, the fact that our metallicities do not show any tendency to vary according to the distance from the SMC center suggests that there is not an age variation either. This is consistent with the possible scenario presented by Piatti et al. (2007c), who derived the age of some outer clusters and found that they are indeed young objects. The lack of a metallicity gradient in our data can also be explained by the presence of a classical bar which tends to weaken the gradient (Zaritsky et al. 1994; Friedli & Benz 1995). This effect has also been seen in the LMC (Olszewski et al. 1991; Geisler et al. 2003; Grocholski et al. 2006).
4. From the comparison between the metallicity of the star fields and that of the clusters they surround, it is evident that there exists a tendency for the fields to be more metal-poor than the clusters, independently of the age of the cluster and of its position in the galaxy. We argue that this is due to the clusters covering a range of both ages and metallicities but mainly younger and more metal-rich, while the field stars may have dated from an older epoch lasting many gigayears in which the metallicity was almost uniform and more metal-poor. Of course, information about the age of the fields is needed to perform a more reliable analysis of the chemical evolution history of field stars and to compare it with the evolution of the cluster system.

The paper was improved by a number of useful comments from the referee. This work is based on observations collected at the European Southern Observatory, Chile, under program number 076.B-0533. We thank the Paranal Science Operations Staff. D.G. gratefully acknowledges support from the Chilean Centro de Astrofísica FONDAP No. 15010003 and the Chilean Centro de Excelencia en Astrofísica y Tecnologías Afines (CATA). M.C.P. and J.J.C. gratefully acknowledge financial support from the Argentinian institutions CONICET, FONCYT, and SECYT (Universidad Nacional de Córdoba).

Facilities: VLT: Antu (FORS2).

REFERENCES

Armandroff, T. E., & Da Costa, G. S. 1991, AJ, 101, 1329
Armandroff, T. E., & Zinn, R. 1988, AJ, 96, 92
Bastian, N., Gieles, M., Ercolano, B., & Gutermuth, R. 2009, MNRAS, 392, 868
Battaglia, G., Irwin, M., Tolstoy, E., Hill, V., Helmi, A., Letarte, B., & Jablonka, P. 2008, MNRAS, 383, 183
Bekki, K., Couch, W. J., Beasley, M. A., Forbes, D. A., Chiba, M., & Da Costa, G. S. 2004, ApJ, 610, L93

Besla, G., Kallivayalil, N., Hernquist, L., Robertson, B., Cox, T. J., van der Marel, R. P., & Alcock, C. 2007, ApJ, 668, 949
Carrera, R., Gallart, C., Aparicio, A., Costa, E., Méndez, R. A., & Noël, N. E. D. 2008, AJ, 136, 1039
Carrera, R., Gallart, C., Pancino, E., & Zinn, R. 2007, AJ, 134, 1298
Carretta, E., & Gratton, R. G. 1997, A&AS, 121, 95
Cenarro, A. J., Gorgas, J., Cardiel, N., Vazdekis, A., & Peletier, R. F. 2002, MNRAS, 329, 863
Chandar, R., Fall, S. M., & Whitmore, B. C. 2006, ApJ, 650, 111
Cioni, M.-R. L. 2009, A&A, 506, 1137
Cole, A. A., Smecker-Hane, T. A., Tolstoy, E., Bosler, T. L., & Gallagher, J. S. 2004, MNRAS, 347, 367 (C04)
Da Costa, G. S., & Hatzidimitriou, D. 1998, AJ, 115, 1934
Dolphin, A. E., Walker, A. R., Hodge, P. W., Mateo, M., Olszewski, E. W., Schommer, R. A., & Suntzeff, N. B. 2001, ApJ, 562, 303
Friedli, D., & Benz, W. 1995, A&A, 301, 649
Friel, E. D., Janes, K. A., Tavarez, M., Scott, J., Katsanis, R., Lotz, J., Hong, L., & Miller, N. 2002, AJ, 124, 2693
Geisler, D., Piatti, A. E., Bica, E., & Clariá, J. J. 2003, MNRAS, 341, 771
Glatt, K., et al. 2008, AJ, 136, 1703
Gonzalez, G., & Wallerstein, G. 1999, AJ, 117, 2286
Grocholski, A. J., Cole, A. A., Sarajedini, A., Geisler, D., & Smith, V. 2006, AJ, 132, 1630
Harris, J., & Zaritsky, D. 2004, AJ, 127, 1531
Harris, J., & Zaritsky, D. 2006, AJ, 131, 2514
Irwin, M., & Tolstoy, E. 2002, MNRAS, 336, 643
Jørgensen, U. G., Carlsson, M., & Johnson, H. R. 1992, A&A, 254, 258
Koch, A., Grebel, E. K., Wyse, R. F. G., Kleyna, J. T., Wilkinson, M. I., Harbeck, D. R., Gilmore, G. F., & Evans, N. W. 2006, AJ, 131, 895
Lada, C. J., & Lada, E. A. 2003, ARA&A, 41, 57
Olszewski, E. W., Schommer, R. A., Suntzeff, N. B., & Harris, H. C. 1991, AJ, 101, 515
Pagel, B. E. J., & Tautvaišienė, G. 1998, MNRAS, 299, 535
Parisi, M. C., Grocholski, A. J., Geisler, D., Sarajedini, A., & Clariá, J. J. 2009, AJ, 138, 517 (Paper I)
Piatti, A. E., Santos, J. F. C., Jr., Clariá, J. J., Bica, E., Sarajedini, A., & Geisler, D. 2001, MNRAS, 325, 792
Piatti, A. E., Sarajedini, A., Geisler, D., Clark, D., & Seguel, J. 2007a, MNRAS, 377, 300
Piatti, A. E., Sarajedini, A., Geisler, D., Gallart, C., & Wischnjewsky, M. 2007b, MNRAS, 381, L84
Piatti, A. E., Sarajedini, A., Geisler, D., Gallart, C., & Wischnjewsky, M. 2007c, MNRAS, 382, 1203
Piatti, A. E., Sarajedini, A., Geisler, D., Seguel, J., & Clark, D. 2005, MNRAS, 358, 1215
Rutledge, G. A., Hesser, J. E., & Stetson, P. B. 1997, PASP, 109, 907
Sabbi, E., et al. 2009, ApJ, 703, 721
Stetson, P. B. 1987, PASP, 99, 191
Tonry, J., & Davis, M. 1979, AJ, 84, 1511
Tsujimoto, T., & Bekki, K. 2009, ApJ, 700, L69
Westerlund, B. E. 1997, The Magellanic Clouds (Cambridge: Cambridge Univ. Press)
Zaritsky, D., Kennicutt, R. C., Jr., & Huchra, J. P. 1994, ApJ, 420, 87